loss of AF5q31 does not cause a complete and uniform block of embryogenesis at a given point but that AF5q31 possesses versatile roles during embryogenesis. Since *AF5q31* and *AF4* are widely expressed during embryogenesis and in the adult tissues of mice, it is possible that AF4 functionally compensates for the lack of AF5q31 in most tissues (4, 33). Presently, it is unclear why the embryonic and neonatal death occurs and whether the incomplete penetrance of this phenotype results from heterogeneity in the genetic background of the mutant mice.

Spermatogenesis is a multistep process from spermatogonia, which are the stem cells of the germ cell lineage, to spermatozoa (14). Sertoli cells play major roles in supporting spermatogenesis, which involves the complex interaction of germ cells and Sertoli cells within the seminiferous tubules (23, 62), and Leydig cells produce the testosterone. The expression of AF5q31 in Sertoli cells without the expression of other family genes in the testis suggests an indispensable role for AF5q31 in the testis. It should be kept in mind that serum levels of testosterone, LH, and FSH and expression levels of *AR*, *LH-R*, and *FSH-R* did not show any significant difference between the wild-type and AF5q31$^{-/-}$ mice. Thus, azoospermia in AF5q31$^{-/-}$ mice seems to be caused by functional defects in testicular somatic cells, particularly Sertoli cells. Several reports suggested that abnormal Sertoli cells were impaired regarding the ability to assist the normal maturation and release of spermatids in the deficient mice for the nuclear receptors and related cofactors such as *RARα*, *RXRβ*, *AR*, and *Cnot7* (10, 15, 30, 36, 40, 48). It is possible that AF5q31 functions as a coregulator of these transcription factors in spermatogenesis.

Human infertility affects 10 to 15% of couples, with an approximately equal contribution from both partners (16). In a large number of male infertility patients, the cause of the infertility might be related to disturbances in the replacement of histones by protamines during spermatogenesis. Previous reports stated that sperm from sterile males shows abnormal protein contents, with anomalously elevated levels of histones and/or an altered protamine 1/2 ratio (3, 11, 17). In mice and humans, genes encoding *Prm1*, *Prm2*, and *TP2* are clustered together on chromosome 16 (52). In addition, these three genes lie in the same orientation to one another and are coordinately expressed in a haploid-specific manner during spermatogenesis. Notwithstanding the subtle decrease of *TP1* expression, the levels of *TP2*, *Prm1*, and *Prm2* were dramatically reduced in AF5q31$^{-/-}$ mice. Previous studies demonstrated that the transcription of transition proteins and protamines initiates shortly after the completion of meiosis in round spermatids (after step 7 in spermiogenesis) and ceases in elongating spermatids (step 11) with a global repression of transcription (37, 42). In addition, the haplo-insufficient chimeras of *Prm1* and *Prm2* were infertile, displaying an abnormal nuclear condensation (12). Thus, the reduced levels of TP2, Prm1, and Prm2 may be the cause of spermiogenesis arrest in AF5q31$^{-/-}$ mice.

Selective decreases in the levels of mRNAs of *TP2*, *Prm1*, and *Prm2* among a set of postmeiotic genes in germ cells raise the possibility that AF5q31 also directly regulates the transcription of these genes. In fact, AF5q31 is weakly expressed in germ cells. It remains to be determined if Sertoli cells and germ cells are independently affected by the lack of AF5q31 or whether germ cells are secondarily affected, or both. Clarification of a potential role for AF5q31 in regulating the expression levels of *TP2*, *Prm1*, and *Prm2* may provide new insights into the mechanisms of human male infertility.

ALLs are characterized by the clonal proliferation, accumulation, and tissue infiltration of neoplastic cells (21). The majority of cases of ALL demonstrate abnormal karyotypes, either in chromosome number or as structural changes such as translocations, inversions, or deletions. As a consequence of translocations between chromosomes 5 and 11, the reciprocal fusion gene is generated and it encodes the MLL-AF5q31 fusion protein, which is expressed in the leukemic blasts (63). It is unknown whether the fusion protein can act as a dominant negative product on AF5q31 function in the leukemic blasts. However, the fact that AF5q31$^{-/-}$ mice did not show any hematological abnormalities suggests that the dominant negative effects of this fusion protein on AF5q31 in leukemogenesis are less likely. It is more likely that MLL-AF5q31 fusion leads to constitutive activation of the MLL target genes (1, 27). Clarification of the AF5q31-mediated gene regulation in testes will also help us to elucidate the molecular mechanism by which the fusion converts normal MLL into the leukemogenic form.

ACKNOWLEDGMENTS

We are grateful to T. Nakamura and T. Noce for useful technical advice and discussions; to M. Sakaki, N. Kakuta, N. Iwamori, J. Kato, and members of the H. Handa laboratory for excellent technical support; and to S. Mori, T. Nakajima, H. Onoda, and N. Oyaizu for invaluable histological analysis. We also thank members of the T. Kitamura laboratory for helpful suggestions.

The Division of Hematopoietic Factors is supported by the Chugai Pharmaceutical Company, Ltd.

REFERENCES

1. **Armstrong, S. A., J. E. Staunton, L. B. Silverman, R. Pieters, M. L. den Boer, M. D. Minden, S. E. Sallan, E. S. Lander, T. R. Golub, and S. J. Korsmeyer.** 2002. MLL translocations specify a distinct gene expression profile that distinguishes a unique leukemia. Nat. Genet. **30**:41–47.
2. **Ayton, P. M., and M. L. Cleary.** 2001. Molecular mechanisms of leukemogenesis mediated by MLL fusion proteins. Oncogene **20**:5695–5707.
3. **Balhorn, R., S. Reed, and N. Tanphaichitr.** 1988. Aberrant protamine 1/protamine 2 ratios in sperm of infertile human males. Experientia **44**:52–55.
4. **Baskaran, K., F. Erfurth, G. Taborn, N. G. Copeland, D. J. Gilbert, N. A. Jenkins, P. M. Iannaccone, and P. H. Domer.** 1997. Cloning and developmental expression of the murine homolog of the acute leukemia protooncogene AF4. Oncogene **15**:1967–1978.
5. **Blendy, J. A., K. H. Kaestner, G. F. Weinbauer, E. Nieschlag, and G. Schutz.** 1996. Severe impairment of spermatogenesis in mice lacking the CREM gene. Nature **380**:162–165.
6. **Bursen, A., S. Moritz, A. Gaussmann, S. Moritz, T. Dingermann, and R. Marschalek.** 2004. Interaction of AF4 wild-type and AF4.MLL fusion protein with SIAH proteins: indication for t(4;11) pathobiology? Oncogene **23**:6237–6249.
7. **Canaani, E., P. C. Nowell, and C. M. Croce.** 1995. Molecular genetics of 11q23 chromosome translocations. Adv. Cancer Res. **66**:213–234.
8. **Chakrabarti, L., S. J. Knight, A. V. Flannery, and K. E. Davies.** 1996. A candidate gene for mild mental handicap at the FRAXE fragile site. Hum. Mol. Genet. **5**:275–282.
9. **Chakrabarti, L., J. Bristulf, G. S. Foss, and K. E. Davies.** 1998. Expression of the murine homologue of FMR2 in mouse brain and during development. Hum. Mol. Genet. **7**:441–448.
10. **Chang, C., Y. T. Chen, S. D. Yeh, Q. Xu, R. S. Wang, F. Guillou, H. Lardy, and S. Yeh.** 2004. Infertility with defective spermatogenesis and hypotestosteronemia in male mice lacking the androgen receptor in Sertoli cells. Proc. Natl. Acad. Sci. USA **101**:6876–6881.
11. **Chevaillier, P., N. Mauro, D. Feneux, P. Jouannet, and G. David.** 1987. Anomalous protein complement of sperm nuclei in some infertile men. Lancet **2**:806–807.
12. **Cho, C., W. D. Willis, E. H. Goulding, H. Jung-Ha, Y. C. Choi, N. B. Hecht, and E. M. Eddy.** 2001. Haploinsufficiency of protamine-1 or -2 causes infertility in mice. Nat. Genet. **28**:82–86.

13. **Collins, E. C., and T. H. Rabbitts.** 2002. The promiscuous MLL gene links chromosomal translocations to cellular differentiation and tumour tropism. Trends Mol. Med. **8:**436–442.
14. **Cooke, H. J., and P. T. Saunders.** 2002. Mouse models of male infertility. Nat. Rev. Genet. **3:**790–801.
15. **De Gendt, K., J. V. Swinnen, P. T. Saunders, L. Schoonjans, M. Dewerchin, A. Devos, K. Tan, N. Atanassova, F. Claessens, C. Lecureuil, W. Heyns, P. Carmeliet, F. Guillou, R. M. Sharpe, and G. Verhoeven.** 2004. A Sertoli cell-selective knockout of the androgen receptor causes spermatogenic arrest in meiosis. Proc. Natl. Acad. Sci. USA **101:**1327–1332.
16. **De Kretser, D. M., and H. W. Baker.** 1999. Infertility in men: recent advances and continuing controversies. J. Clin. Endocrinol. Metab. **84:**3443–3450.
17. **de Yebra, L., J. L. Ballesca, J. A. Vanrell, L. Bassas, and R. Oliva.** 1993. Complete selective absence of protamine P2 in humans. J. Biol. Chem. **268:**10553–10557.
18. **Djabali, M., L. Selleri, P. Parry, M. Bower, B. D. Young, and G. A. Evans.** 1992. A trithorax-like gene is interrupted by chromosome 11q23 translocations in acute leukaemias. Nat. Genet. **2:**113–118.
19. **Domer, P. H., S. S. Fakharzadeh, C. S. Chen, J. Jockel, L. Johansen, G. A. Silverman, J. H. Kersey, and S. J. Korsmeyer.** 1993. Acute mixed-lineage leukemia t(4;11)(q21;q23) generates an MLL-AF4 fusion product. Proc. Natl. Acad. Sci. USA **90:**7884–7888.
20. **Estable, M. C., M. H. Naghavi, H. Kato, H. Xiao, J. Qin, A. Vahlne, and R. G. Roeder.** 2002. MCEF, the newest member of the AF4 family of transcription factors involved in leukemia, is a positive transcription elongation factor-b-associated protein. J. Biomed. Sci. **9:**234–245.
21. **Faderl, S., H. M. Kantarjian, M. Talpaz, and Z. Estrov.** 1998. Clinical significance of cytogenetic abnormalities in adult acute lymphoblastic leukemia. Blood **91:**3995–4019.
22. **Gecz, J., A. K. Gedeon, G. R. Sutherland, and J. C. Mulley.** 1996. Identification of the gene FMR2, associated with FRAXE mental retardation. Nat. Genet. **13:**105–108.
23. **Griswold, M. D.** 1995. Interactions between germ cells and Sertoli cells in the testis. Biol. Reprod. **52:**211–216.
24. **Gu, Y., T. Nakamura, H. Alder, R. Prasad, O. Canaani, G. Cimino, C. M. Croce, and E. Canaani.** 1992. The t(4;11) chromosome translocation of human acute leukemias fuses the ALL-1 gene, related to Drosophila trithorax, to the AF-4 gene. Cell **71:**701–708.
25. **Gu, Y., Y. Shen, R. A. Gibbs, and D. L. Nelson.** 1996. Identification of FMR2, a novel gene associated with the FRAXE CCG repeat and CpG island. Nat. Genet. **13:**109–113.
26. **Guerif, F., V. Cadoret, M. Plat, M. Magistrini, J. Lansac, M. T. Hochereau-De Reviers, and D. Royere.** 2002. Characterization of the fertility of Kit haplodeficient male mice. Int. J. Androl. **25:**358–368.
27. **Hess, J. L.** 2004. MLL: a histone methyltransferase disrupted in leukemia. Trends Mol. Med. **10:**500–507.
28. **Hillman, M. A., and J. Gecz.** 2001. Fragile XE-associated familial mental retardation protein 2 (FMR2) acts as a potent transcription activator. J. Hum. Genet. **46:**251–259.
29. **Hiwatari, M., T. Taki, T. Taketani, M. Taniwaki, K. Sugita, M. Okuya, M. Eguchi, K. Ida, and Y. Hayashi.** 2003. Fusion of an AF4-related gene, LAF4, to MLL in childhood acute lymphoblastic leukemia with t(2;11)(q11;q23). Oncogene **22:**2851–2855.
30. **Holdcraft, R. W., and R. E. Braun.** 2004. Androgen receptor function is required in Sertoli cells for the terminal differentiation of haploid spermatids. Development **131:**459–467.
31. **Huret, J. L., P. Dessen, and A. Bernheim.** 2001. An atlas of chromosomes in hematological malignancies. Example: 11q23 and MLL partners. Leukemia **15:**987–989.
32. **Isaacs, A. M., P. L. Oliver, E. L. Jones, A. Jeans, A. Potter, B. H. Hovik, P. M. Nolan, L. Vizor, P. Glenister, A. K. Simon, I. C. Gray, N. K. Spurr, S. D. Brown, A. J. Hunter, and K. E. Davies.** 2003. A mutation in Af4 is predicted to cause cerebellar ataxia and cataracts in the robotic mouse. J. Neurosci. **23:**1631–1637.
33. **Isnard, P., D. Depetris, M. G. Mattei, P. Ferrier, and M. Djabali.** 1998. cDNA cloning, expression and chromosomal localization of the murine AF-4 gene involved in human leukemia. Mamm. Genome **9:**1065–1068.
34. **Isnard, P., N. Core, P. Naquet, and M. Djabali.** 2000. Altered lymphoid development in mice deficient for the mAF4 proto-oncogene. Blood **96:**705–710.
35. **Kashiwabara, S., J. Noguchi, T. Zhuang, K. Ohmura, A. Honda, S. Sugiura, K. Miyamoto, S. Takahashi, K. Inoue, A. Ogura, and T. Baba.** 2002. Regulation of spermatogenesis by testis-specific, cytoplasmic poly(A) polymerase TPAP. Science **298:**1999–2002.
36. **Kastner, P., M. Mark, M. Leid, A. Gansmuller, W. Chin, J. M. Grondona, D. Decimo, W. Krezel, A. Dierich, and P. Chambon.** 1996. Abnormal spermatogenesis in RXR beta mutant mice. Genes Dev. **10:**80–92.
37. **Kierszenbaum, A. L., and L. L. Tres.** 1975. Structural and transcriptional features of the mouse spermatid genome. J. Cell Biol. **65:**258–270.
38. **Kurohmaru, M., Y. Kanai, and Y. Hayashi.** 1992. A cytological and cytoskeletal comparison of Sertoli cells without germ cell and those with germ cells using the W/W^{v} mutant mouse. Tissue Cell **24:**895–903.
39. **Kuzin, B., S. Tillib, Y. Sedkov, L. Mizrokhi, and A. Mazo.** 1994. The Drosophila trithorax gene encodes a chromosomal protein and directly regulates the region-specific homeotic gene fork head. Genes Dev. **8:**2478–2490.
40. **Lufkin, T., D. Lohnes, M. Mark, A. Dierich, P. Gorry, M. P. Gaub, M. LeMeur, and P. Chambon.** 1993. High postnatal lethality and testis degeneration in retinoic acid receptor alpha mutant mice. Proc. Natl. Acad. Sci. USA **90:**7225–7229.
41. **Ma, C., and L. M. Staudt.** 1996. LAF-4 encodes a lymphoid nuclear protein with transactivation potential that is homologous to AF-4, the gene fused to MLL in t(4;11) leukemias. Blood **87:**734–745.
42. **Mali, P., A. Kaipia, M. Kangasniemi, J. Toppari, M. Sandberg, N. B. Hecht, and M. Parvinen.** 1989. Stage-specific expression of nucleoprotein mRNAs during rat and mouse spermiogenesis. Reprod. Fertil. Dev. **1:**369–382.
43. **Martianov, I., G. M. Fimia, A. Dierich, M. Parvinen, P. Sassone-Corsi, and I. Davidson.** 2001. Late arrest of spermiogenesis and germ cell apoptosis in mice lacking the TBP-like TLF/TRF2 gene. Mol. Cell **7:**509–515.
44. **Mazo, A. M., D. H. Huang, B. A. Mozer, and I. B. Dawid.** 1990. The trithorax gene, a trans-acting regulator of the bithorax complex in Drosophila, encodes a protein with zinc-binding domains. Proc. Natl. Acad. Sci. USA **87:**2112–2116.
45. **Milne, T. A., S. D. Briggs, H. W. Brock, M. E. Martin, D. Gibbs, C. D. Allis, and J. L. Hess.** 2002. MLL targets SET domain methyltransferase activity to Hox gene promoters. Mol. Cell **10:**1107–1117.
46. **Morrissey, J., D. C. Tkachuk, A. Milatovich, U. Francke, M. Link, and M. L. Cleary.** 1993. A serine/proline-rich protein is fused to HRX in t(4;11) acute leukemias. Blood **81:**1124–1131.
47. **Mozer, B. A., and I. B. Dawid.** 1989. Cloning and molecular characterization of the trithorax locus of Drosophila melanogaster. Proc. Natl. Acad. Sci. USA **86:**3738–3742.
48. **Nakamura, T., R. Yao, T. Ogawa, T. Suzuki, C. Ito, N. Tsunekawa, K. Inoue, R. Ajima, T. Miyasaka, Y. Yoshida, A. Ogura, K. Toshimori, T. Noce, T. Yamamoto, and T. Noda.** 2004. Oligo-astheno-teratozoospermia in mice lacking Cnot7, a regulator of retinoid X receptor beta. Nat. Genet. **36:**528–533.
49. **Nakamura, T., H. Alder, Y., Gu, R. Prasad, O. Canaani, N. Kamada, R. P. Gale, B. Lange, W. M. Crist, and P. C. Nowell.** 1993. Genes on chromosomes 4, 9, and 19 involved in 11q23 abnormalities in acute leukemia share sequence homology and/or common motifs. Proc. Natl. Acad. Sci. USA **90:**4631–4635.
50. **Nakamura, T., T. Mori, S. Tada, W. Krajewski, T. Rozovskaia, R. Wassell, G. Dubois, A. Mazo, C. M. Croce, and E. Canaani.** 2002. ALL-1 is a histone methyltransferase that assembles a supercomplex of proteins involved in transcriptional regulation. Mol. Cell **10:**1119–1128.
51. **Nantel, F., L. Monaco, N. S. Foulkes, D. Masquilier, M. LeMeur, K. Henriksen, A. Dierich, M. Parvinen, and P. Sassone-Corsi.** 1996. Spermiogenesis deficiency and germ-cell apoptosis in CREM-mutant mice. Nature **380:**159–162.
52. **Nelson, J. E., and S. A. Krawetz.** 1993. Linkage of human spermatid-specific basic nuclear protein genes. Definition and evolution of the P1→P2→TP2 locus. J. Biol. Chem. **268:**2932–2936.
53. **Nilson, I., M. Reichel, M. G. Ennas, R. Greim, C. Knorr, G. Siegler, J. Greil, G. H. Fey, and R. Marschalek.** 1997. Exon/intron structure of the human AF-4 gene, a member of the AF-4/LAF-4/FMR-2 gene family coding for a nuclear protein with structural alterations in acute leukaemia. Br. J. Haematol. **98:**157–169.
54. **Nosaka, T., J. M. van Deursen, R. A. Tripp, W. E. Thierfelder, B. A. Witthuhn, A. P. McMickle, P. C. Doherty, G. C. Grosveld, and J. N. Ihle.** 1995. Defective lymphoid development in mice lacking Jak3. Science **270:**800–802.
55. **Nosaka, T., S. Morita, H. Kitamura, H. Nakajima, F. Shibata, Y. Morikawa, Y. Kataoka, Y. Ebihara, T. Kawashima, T. Itoh, K. Ozaki, E. Senba, K. Tsuji, F. Makishima, N. Yoshida, and T. Kitamura.** 2003. Mammalian twisted gastrulation is essential for skeleto-lymphogenesis. Mol. Cell. Biol. **23:**2969–2980.
56. **Nosaka, T., T. Kawashima, K. Misawa, K. Ikuta, A. L.-F. Mui, and T. Kitamura.** 1999. STAT5 as a molecular regulator of proliferation, differentiation and apoptosis in hematopoietic cells. EMBO J. **18:**4654–4765.
57. **Oliver, P. L., E. Bitoun, J. Clark, E. L. Jones, and K. E. Davies.** 2004. Mediation of Af4 protein function in the cerebellum by Siah proteins. Proc. Natl. Acad. Sci. USA **101:**14901–14906.
58. **Prasad, R., T. Yano, C. Sorio, T. Nakamura, R. Rallapalli, Y. Gu, D. Leshkowitz, C. M. Croce, and E. Canaani.** 1995. Domains with transcriptional regulatory activity within the ALL1 and AF4 proteins involved in acute leukemia. Proc. Natl. Acad. Sci. USA **92:**12160–12164.
59. **Rabbitts, T. H.** 1994. Chromosomal translocations in human cancer. Nature **372:**143–149.
60. **Rowley, J. D.** 2001. Chromosome translocations: dangerous liaisons revisited. Nat. Rev. Cancer **1:**245–250.
61. **Sassone-Corsi, P.** 2002. Unique chromatin remodeling and transcriptional regulation in spermatogenesis. Science **296:**2176–2178.
62. **Siu, M. K., and C. Y. Cheng.** 2004. Dynamic cross-talk between cells and the extracellular matrix in the testis. Bioessays **26:**978–992.
63. **Taki, T., H. Kano, M. Taniwaki, M. Sako, M. Yanagisawa, and Y. Hayashi.**

1999. AF5q31, a newly identified AF4-related gene, is fused to MLL in infant acute lymphoblastic leukemia with ins(5;11)(q31;q13q23). Proc. Natl. Acad. Sci. USA **96:**14535–14540.

64. **Tkachuk, D. C., S. Kohler, and M. L. Cleary.** 1992. Involvement of a homolog of Drosophila trithorax by 11q23 chromosomal translocations in acute leukemias. Cell **7:**691–700.
65. **von Bergh, A. R., H. B. Beverloo, P. Rombout, E. R. van Wering, M. H. van Weel, G. C. Beverstock, P. M. Kluin, R. M. Slater, and E. Schuuring.** 2002. LAF4, an AF4-related gene, is fused to MLL in infant acute lymphoblastic leukemia. Genes Chromosomes Cancer **35:**92–96.
66. **Wada, T., T. Takagi, Y. Yamaguchi, A. Ferdous, T. Imai, S. Hirose, S. Sugimoto, K. Yano, G. A. Hartzog, F. Winston, S. Buratowski, and H. Handa.** 1998. DSIF, a novel transcription elongation factor that regulates RNA polymerase II processivity, is composed of human Spt4 and Spt5 homologs. Genes Dev. **12:**343–356.
67. **Wada, T., T. Takagi, Y. Yamaguchi, D. Watanabe, and H. Handa.** 1998. Evidence that P-TEFb alleviates the negative effect of DSIF on RNA polymerase II-dependent transcription in vitro. EMBO J. **17:**7395–7403.
68. **Wu, J. Y., and A. R. Means.** 2000. Ca(2+)/calmodulin-dependent protein kinase IV is expressed in spermatids and targeted to chromatin and the nuclear matrix. J. Biol. Chem. **275:**7994–7999.
69. **Wu, J. Y., T. J. Ribar, D. E. Cummings, K. A. Burton, G. S. McKnight, and A. R. Means.** 2000. Spermiogenesis and exchange of basic nuclear proteins are impaired in male germ cells lacking Camk4. Nat. Genet. **25:**448–452.
70. **Yokoyama, A., Z. Wang, J. Wysocka, M. Sanyal, D. J. Aufiero, I. Kitabayashi, W. Herr, and M. L. Cleary.** 2004. Leukemia proto-oncoprotein MLL forms a SET1-like histone methyltransferase complex with menin to regulate *Hox* gene expression. Mol. Cell. Biol. **24:**5639–5649.
71. **Yomogida, K., H. Ohtani, H. Harigae, E. Ito, Y. Nishimune, J. D. Engel, and M. Yamamoto.** 1994. Developmental stage- and spermatogenic cycle-specific expression of transcription factor GATA-1 in mouse Sertoli cells. Development **120:**1759–1766.
72. **Yu, B. D., J. L. Hess, S. E. Horning, G. A. Brown, and S. J. Korsmeyer.** 1995. Altered Hox expression and segmental identity in Mll-mutant mice. Nature **378:**505–508.
73. **Yu, B. D., R. D. Hanson, J. L. Hess, S. E. Horning, and S. J. Korsmeyer.** 1998. MLL, a mammalian trithorax-group gene, functions as a transcriptional maintenance factor in morphogenesis. Proc. Natl. Acad. Sci. USA **95:**10632–10636.
74. **Zhang, D., T. L. Penttila, P. L. Morri, M. Teichmann, and R. G. Roeder.** 2001. Spermiogenesis deficiency in mice lacking the Trf2 gene. Science **292:**1153–1155.

Physiologic Assessment of Coronary Artery Stenosis without Stress Tests: Noninvasive Analysis of Phasic Flow Characteristics by Transthoracic Doppler Echocardiography

Masao Daimon, MD, Hiroyuki Watanabe, MD, Hiroyuki Yamagishi, MD, Yoichi Kuwabara, MD, Rei Hasegawa, MD, Tomohiko Toyoda, MD, Katsuya Yoshida, MD, PhD, Junichi Yoshikawa, MD, PhD, and Issei Komuro, MD, PhD, *Chiba, and Osaka, Japan*

We evaluated the significance of the diastolic-to-systolic blood flow velocity ratio (DSVR) determined by transthoracic Doppler echocardiography, for a physiologic assessment of the severity of coronary stenosis without stress tests, as compared with thallium 201 single photon emission computed tomography. In 95 patients undergoing thallium 201 single photon emission computed tomography for coronary artery disease, the flow velocity in the distal left anterior descending coronary artery was obtained with transthoracic Doppler echocardiography. The mean and peak DSVR values were calculated using mean and peak coronary flow velocity. DSVR was successfully measured for 82 patients (86.3%), including 33 patients with reversible perfusion defects in the left anterior descending coronary artery territories. For predicting reversible perfusion defects in thallium 201 single photon emission computed tomography, the best cut-off points were 1.5 for mean DSVR (sensitivity 81.8%, specificity 85.7%) and 1.6 for peak DSVR (sensitivity 75.7%, specificity 83.6%). Noninvasive measurement of DSVR with transthoracic Doppler echocardiography provides physiologic estimation of the left anterior descending coronary artery stenosis severity at high success rate, without stress tests. (J Am Soc Echocardiogr 2005;18:949-955.)

Coronary angiography is the currently accepted standard method for assessing coronary artery disease. However, several clinical reports have pointed out discrepancies between angiographic and physiologic estimates of coronary lesion severity.[1-3] Thus, some form of stress testing is often required to detect critical coronary stenosis.

Coronary blood flow velocity analyses have been proposed to allow additional evaluation of coronary artery stenosis, including the diastolic-to-systolic blood flow velocity ratio (DSVR), proximal/distal blood flow velocity ratio, and the coronary blood flow velocity reserve.[4-12] Despite the clinical usefulness of those parameters, they have been assessed mainly by invasive intracoronary Doppler guidewire and their clinical use is, therefore, generally restricted. It was recently reported that DSVR in the distal left anterior descending coronary artery (LAD), one of the coronary blood flow measurements available without stress tests, could be assessed by totally noninvasive transthoracic Doppler echocardiography (TTDE) with technologic advancement, and was useful for detecting angiographic severe stenosis in the LAD.[13-15] However, DSVR determined by TTDE has not been evaluated sufficiently to determine its usefulness for the physiologic assessment of the severity of coronary artery stenosis.

In this study, we evaluated the value of DSVR as determined by TTDE, for the physiologic assessment of the severity of coronary stenosis without stress tests, in comparison with exercise thallium 201 single photon emission computed tomography (Tl-SPECT). In addition, several recent reports have shown that contrast-enhanced Doppler echocardiography has a high success rate in the evaluation of coronary blood flow noninvasively.[16,17] We also evaluated the effect of contrast enhancement on improvement of measuring DSVR by high-frequency TTDE.

From the Department of Cardiovascular Science and Medicine, Chiba University, Graduate School of Medicine, and Department of Internal Medicine and Cardiology, Osaka City University, Graduate School of Medicine (H.W., H.Y., J.Y.).

Reprint requests: Issei Komuro, MD, PhD, Department of Cardiovascular Science and Medicine, Chiba University, Graduate School of Medicine, Inohana 1-8-1, Chuo-ku, Chiba City, Chiba 260-8670, Japan (E-mail: *komuro-tky@umin.ac.jp*).

0894-7317/$30.00

doi:10.1016/j.echo.2005.01.006

METHODS

Patient Population

We prospectively enrolled 95 consecutive patients (mean age 63 ± 9 years; 78 men and 17 women) who had been admitted to our hospital for assessment of coronary artery disease. Exclusion criteria were previous myocardial infarction, previous cardiac operation, artificial pacemaker, nonsinus rhythm, significant valvular heart disease, angina at rest, chronic obstructive pulmonary disease, and congestive heart failure. All patients continued administration of anti-ischemic medication (nitrates, β-blockers, calcium antagonists) and antiplatelet agents (aspirin, 81 mg) on the day of the echocardiographic study. On 2-dimensional echocardiography, none had evidence of left ventricular wall-motion abnormality, left ventricular hypertrophy (wall thickness at end diastole >12 mm), or valvular heart disease. All patients underwent Tl-SPECT and coronary angiography within 1 week of the echocardiographic study. Informed consent was obtained from all patients included in the study. The protocol was approved by our hospital committee on medical ethics and clinical investigation.

TTDE

Echocardiography was performed with a digital ultrasound system (Sequoia 512, Siemens, Mountain View, Calif) using a high-frequency transducer (5-7 MHz). For color Doppler echocardiography, velocity was set in the range of ± 12.0 to ± 24.0 cm/s. Adequate filtering was used to minimize low-frequency wall-motion artifacts. Echocardiographic images were obtained from the acoustic window around the midclavicular line in the fourth and fifth intercostal spaces in the left lateral decubitus position. After the lower portion of the interventricular sulcus had been located in the long-axis cross section, the ultrasound beam was rotated laterally, visualizing the distal portion of LAD under color flow mapping guidance.[18] Color flow of LAD was visualized by high-frequency (3.5-MHz) color Doppler technique. Blood flow velocity was measured by pulsed wave Doppler (Doppler frequency 3.5 MHz) using a sample volume (2.0-3.0 mm) placed on the color signal in the distal LAD. We tried to align the ultrasound beam direction to the distal LAD flow in as parallel a manner as possible. In addition, it has been known that coronary blood flow can be accelerated locally at stenotic sites, and this accelerated coronary flow velocity could lead to the error in DSVR measurements. On the other hand, it has also been reported that localized aliasing, which reflects increased velocity over the velocity range, could be displayed at the stenotic sites in the coronary artery by color flow mapping,[19] even with nonsignificant stenosis (< 50%). Therefore, in the cases with localized color aliasing in LAD, we put the sample volume at the distal site to the aliasing, to avoid the error in DSVR measurements because of local accelerated coronary flow. All studies were continuously recorded on .5-in super-VHS videotape, and clips of stopped frames were also stored digitally on magneto-optical disks (230 MB) for offline analysis. Blood pressure and heart rate were recorded simultaneously.

Echocardiographic Contrast Enhancement

In cases where visualization of the color signals in LAD was unsuccessful or Doppler spectral tracing of velocity was not clear, an echocardiographic contrast agent (Levovist, Tanabe Seiyaku Inc, Osaka, Japan, and Schering, Berlin, Germany) was used to improve visualization of color Doppler signals and obtain clear spectral Doppler signals. On the basis of the results of previous studies,[16,17] contrast agent at 300 mg/mL was infused intravenously to a total volume of 7 mL at a rate of 1 mL/min by infusion pump during coronary blood flow velocity measurements. The infusion rate was adjusted in a range from 0.5 to 2.0 mL/min depending on the quality of the Doppler signal enhancement achieved.

Analysis of Coronary Flow Velocity Characteristics

An experienced operator with no knowledge of the results of Tl-SPECT and coronary angiography assessed DSVR. Measurements of blood flow velocity were performed offline using the integrated evaluation program in the ultrasound system. Four parameters were measured by tracing the contour of the Doppler velocity pattern: (1) mean systolic velocity; (2) mean diastolic velocity; (3) peak systolic velocity; and (4) peak diastolic velocity. Values for each parameter were obtained by averaging measurements from 3 consecutive cardiac cycles. Mean and peak DSVRs were computed as the ratios of diastolic-to-systolic mean and peak coronary flow velocities.

Exercise Tl-SPECT

Tl-SPECT was performed within 1 week of the echocardiographic studies by TTDE. All patients performed symptom-limited exercise on a bicycle ergometer in the sitting position. Nitrates, β-blockers, and calcium channel blockers were withheld on the morning of the test. Twelve-lead electrocardiograms and blood pressure measurements were obtained at baseline and every minute during exercise. The initial workload was 50 W, which was increased by 25 W every 2 minutes until an end point was reached. The end points included excessive fatigue, dyspnea, dizziness, angina, hypotension, diagnostic S-T segment depression (> 1.5 mm horizontal or downsloping or > 2.0 mm upsloping), or significant arrhythmia. At peak exercise a dose of 111 MBq of Tl-201 was injected intravenously. The initial images were obtained immediately after the termination of exercise, and delayed images were obtained 4 hours later.

Single-photon emission computed tomography was performed using a single-head gamma scintillation camera equipped with a low-energy, all-purpose, parallel-hole collimator. A total of 32 equidistant projections were acquired over 180 degrees from the right anterior oblique to the left posterior oblique view at 25 s/projection.

On the Tl-SPECT images, anteroseptal and apical segments were considered to be in the LAD territory. The images were analyzed individually by two experienced nuclear physicians who had no knowledge of the angiographic or echocardiographic data. Disagreements in interpretation were resolved by consensus of the two physicians. The patients were considered to have myocardial ischemia when Tl-SPECT revealed perfusion defects with redistribution on delayed imaging.

Coronary Angiography

Coronary angiography was performed in all patients using standard techniques within 1 week of echocardiographic studies by TTDE. Angiographic data were subsequently analyzed by an experienced investigator who had no knowledge of the echocardiographic or Tl-SPECT results. The severity of coronary stenosis was visually determined and expressed as the percent lumen diameter. Stenosis was considered significant if there was more than 50% diameter stenosis in at least one projection. Electrical calipers were used when necessary.

Statistical Analysis

On the basis of the Tl-SPECT data for the LAD territories, the study patients were classified into group A with abnormal perfusion and group B with normal perfusion. Parametric data were presented as mean ± SD. Categoric variables were compared using Fisher exact test. Mean and peak DSVR values for groups A and B were compared by unpaired *t* test. For all analyses, $P < .05$ was considered significant. For mean and peak DSVRs, sensitivity and specificity, as predictors of abnormal perfusion in Tl-SPECT, were determined for ratio values (in 0.1 increments) between 1.0 and 2.0, with determination of ratio cut-off values yielding the highest combined sensitivity and specificity values. The positive and negative predictive values of DSVR for determination of the presence of abnormal perfusion in Tl-SPECT were determined in the traditional manner.

RESULTS

Effect of Contrast Enhancement on Coronary Flow Velocity Measurements

Of the 95 study patients, adequate spectral Doppler recordings of coronary flow through both systole and diastole in distal LAD were obtained for 82 patients (86.3%), including 14 patients given an echocardiographic contrast agent to improve spectral Doppler signals. The use of contrast enhancement improved the feasibility of spectral Doppler recording with high-frequency TTDE in LAD from 71.6% to 86.3% (Figure 1). In the other 13 patients DSVR measurements could not be obtained because of obscure color Doppler signal (3 patients) or spectral Doppler recordings of only diastole (10 patients), even with contrast enhancement, and they were excluded from the study. Therefore, 82 patients comprised the study group in which we compared echocardiographic data with Tl SPECT results.

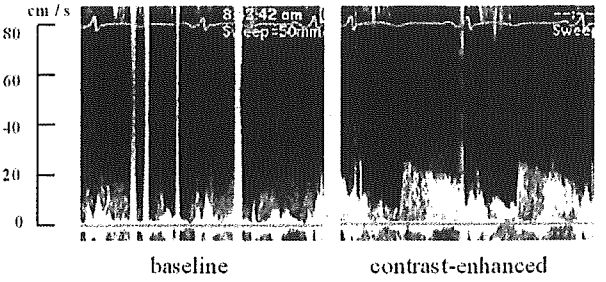

Figure 1 Use of contrast enhancement improved spectral Doppler signal recording in left anterior descending coronary artery (**B**) in case with poor Doppler signals (**A**).

Tl-SPECT

All patients in this study performed exercise tests until the end points. Of the 82 patients, 33 qualitatively exhibited abnormal perfusion in the LAD territories on Tl-SPECT and were classified into group A. The remaining patients (n = 49) had normal perfusion (n = 34) or abnormal perfusion in other territories (n = 15) and were, thus, classified into group B (49 patients). The peak heart rate and rate-pressure product were similar in groups A and B for all exercise tests. No significant difference was found in terms of age, sex, heart rate, and systemic blood pressure between groups A and B (Table 1).

Coronary Angiography

Coronary angiography demonstrated significant coronary stenosis from mid- to proximal LAD of all 33 patients of group A, and in 15 patients of group B. Of the 13 patients who could not undergo Doppler recording, two had total occlusion in the proximal LAD, with good collateral flow from the right coronary artery.

DSVR Measured by TTDE Versus Tl-SPECT

There were no significant differences in both mean and peak systolic flow velocities between groups A and B (Table 2). However, both mean and peak diastolic velocities were significantly smaller in group A than in group B (16.3 ± 5.2 vs 19.8 ± 6.7 cm/s and 20.7 ± 6.5 vs 25.0 ± 9.1 cm/s, $P < .05$, respectively) (Table 2). Thus, there were significant differences in both mean DSVR and peak DSVR between groups A and B (1.4 ± 0.4 vs 1.9 ± 0.6 and 1.4 ± 0.4 vs 2.0 ± 0.5, $P < .0001$, respectively) (Table 2; Figure 2).

For determination of physiologic stenosis in LAD by Tl-SPECT (abnormal perfusion), the sensitivity

Table 1 Clinical data

	Group A (N = 33)	Group B (N = 49)
Age, y	63 ± 8	62 ± 11
Sex, M/F	28/5	38/11
SBP, mm Hg	129 ± 25	123 ± 21
DBP, mm Hg	71 ± 13	69 ± 12
HR, beats/min	58 ± 11	61 ± 12

DBP, Diastolic blood pressure; *F,* female; *HR,* heart rate; *M,* male; *SBP,* systolic blood pressure.Data presented are mean value ± SD or No. of patients.

Table 2 Coronary flow velocity and diastolic-to-systolic flow velocity ratio

	Group A	Group B
MCFV, cm/s		
Systolic	11.7 ± 3.7	10.9 ± 3.9
Diastolic	16.3 ± 5.2	19.8 ± 6.7*
PCFV, cm/s		
Systolic	14.1 ± 4.5	13.4 ± 5.5
Diastolic	20.7 ± 6.5	25.0 ± 9.1*
DSVR		
Mean	1.4 ± 0.4	1.9 ± 0.6†
Peak	1.4 ± 0.4	2.0 ± 0.5†

DSVR, Diastolic-to-systolic flow velocity ratio; *MCFV,* mean coronary flow velocity; *PCFV,* peak coronary flow velocity.
*$P < .05$ vs. group A; †$P < .0001$ vs group A.

and specificity curves for the mean and peak DSVRs were obtained and shown in Figure 3. The best cut-off points were 1.5 for mean DSVR (sensitivity 81.8%, specificity 85.7%, positive predictive value 79.4%, negative predictive value 87.5%) and 1.6 for peak DSVR (sensitivity 75.7%, specificity 83.6%, positive predictive value 75.7%, negative predictive value 83.6%).

Observer Variability

Interobserver and intraobserver variabilities for measurement of Doppler velocity recording were 5.0% and 3.9%, respectively.

DISCUSSION

This study demonstrated that measurement of DSVR by TTDE permits noninvasive and physiologic assessment of the severity of LAD stenosis and prediction of myocardial ischemia in comparison with the value obtained by exercise myocardial perfusion imaging results. It also showed that the combination of contrast enhancement and high-frequency transducer has a high success rate in the noninvasive measurement of DSVR by TTDE.

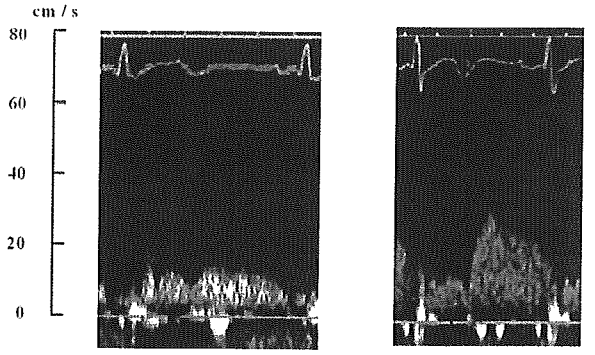

Figure 2 Examples of spectral Doppler signals for patients with abnormal (*left*) and normal (*right*) perfusion in left anterior descending coronary artery territories.

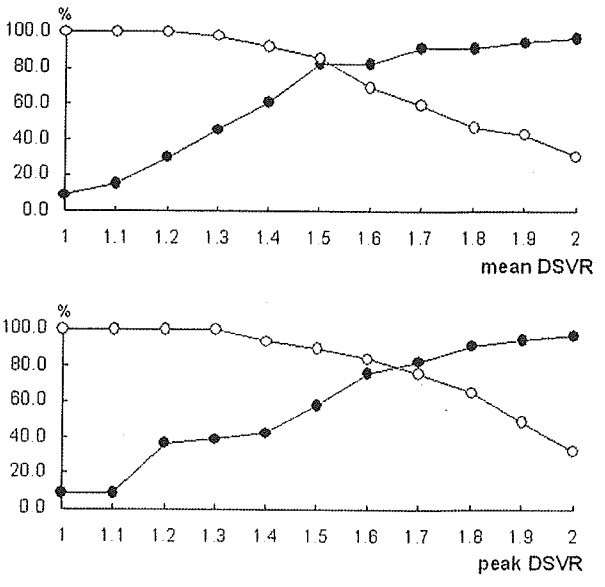

Figure 3 Sensitivity (*open circles*) and specificity (*closed circles*) as functional cut-off values over whole spectrum of mean (*top*) and peak (*bottom*) diastolic-to-systolic blood flow velocity ratio (DSVR). Best cut-off points were 1.5 for mean DSVR (sensitivity, 81.8%; specificity, 85.7%) and 1.6 for peak DSVR (sensitivity, 75.7%; specificity, 83.6%).

Physiologic Assessment of Coronary Stenosis by TTDE

Experimental studies have indicated that coronary blood flow at rest generally can be maintained in coronary stenosis with the severity of less than 85% by autoregulation mechanism.[20,21] However, coronary angiography has limited reliability in predicting the physiologic significance of coronary artery stenosis in the clinical stetting.[1-3] Even an anatomic quantitative intravascular ultrasound has been reported to lack power to predict the physiologic response of coronary stenosis.[22] Thus, clinical decisions concerning the presence of myocardial isch-

emia depended mainly on diagnostic information from stress tests such as the radionuclide stress test or stress echocardiography. This discrepancy between angiographic and physiologic estimates of coronary lesion severity led to research into the evaluation of coronary hemodynamics using the invasive Doppler guidewire.

This study is the first to report that the evaluation of noninvasive measurement of DSVR by TTDE may reveal the physiologic severity of coronary stenosis in the clinical setting, as confirmed by a previous report that the phasic coronary flow pattern was altered with increasing amounts of fixed partial obstruction, and DSVR was decreased as percent stenosis was increased in an experimental study.[4]

Our predictive value of 1.5 for mean DSVR (sensitivity 81.8% and specificity 85.7%) and 1.6 for peak DSVR (sensitivity 75.7% and specificity 83.6%) for physiologic significance of coronary stenosis are higher compared with a previous report in which DSVR by TTDE was compared with angiographic 85% stenosis (1.5 for mean DSVR, sensitivity 77.0% and specificity 77.9%; 1.6 for peak DSVR, sensitivity 79.0% and specificity 75.7%).[15] Despite autoregulation of coronary blood flow suggested by experimental studies,[20,21] a number of studies have shown altered poststenotic phasic coronary blood flow pattern,[4-15] sometimes even in moderate coronary artery stenosis less than 85% obstruction.[10,11,14] Furthermore, some have indicated that altered poststenotic phasic coronary blood flow patterns can reflect the results of some form of examinations for physiologic assessment of coronary stenosis.[10,11,14] These facts support the concept that angiography has limited reliability in predicting physiologic significance of coronary stenosis, and are consistent with our results.

Comparison with Previous Methods

Recently, we reported that measurement of coronary flow reserve by TTDE provides physiologic information on the severity of coronary stenosis equivalent to that obtained with Tl-SPECT with a high success rate (92%).[23] As a matter of fact, coronary flow reserve is a better predictor than DSVR measurement, as indicated in that previous report.[23] Furthermore, a higher success rate could be achieved in the measurement of coronary flow reserve than in that of DSVR because of the difficulty in recording systolic blood flow with TTDE,[16] as also shown in the current study where the recording of diastolic blood flow only was obtained in 10 of the patients. However, the fact that measurement of DSVR by TTDE does not require any pharmacologic stress, which is associated with atrioventricular block, systemic hypotension, and dyspnea,[24] represents an important advantage in addition to the fact that it is an absolutely noninvasive procedure. To our knowledge, no previous studies have reported any other modalities applicable in the clinical setting that allow functional estimates of the severity of coronary stenosis, without hemodynamic monitoring or stress test, besides our method.

Coronary Flow Velocity Measurements with Contrast-enhanced TTDE

In this study, we measured spectral Doppler recordings of coronary flow through both the systole and diastole in distal LAD with a high success rate (86.3%), sufficient for application in the clinical setting, using contrast-enhanced Doppler recording and a high-frequency transducer. Measurement of DSVR by TTDE is the only noninvasive method for assessing the severity of coronary stenosis, without any specific stress testing, available in the clinical setting thus far. However, its success rate was often not high enough to allow its clinical use. These days, technical advancements in Doppler echocardiography, including second-harmonic Doppler imaging and contrast-enhanced Doppler imaging, have enabled us to assess coronary blood flow noninvasively with a high success rate. In particular, contrast enhancement has proved to be useful in increasing the Doppler signal-to-noise ratio in coronary artery by increasing the amplitude of the signal[25,26] and in detecting color Doppler signals in LAD with second-harmonic technology.[16,17]

On the other hand, a high-frequency transducer also has been known to be useful for assessing diastolic coronary blood flow with a high success rate.[18,23,27] This study demonstrated that the combination of contrast enhancement and high-frequency transducer also allows the noninvasive assessment of coronary blood flow velocity through both systole and diastole by TTDE.

Study Limitations

First, there were still some cases in which it was difficult to obtain complete Doppler spectral envelopes throughout the entire cardiac cycle. However, as can be expected from recent studies, further technical advancements will result in even higher success rates for this noninvasive method of DSVR measurement in the near future.

In this study, the angle between the Doppler beam and the artery was quite large (> 30 degrees) in a certain number of cases, causing underestimation of the true flow velocity. However, for the purpose of DSVR evaluation, the absolute velocity value was not needed because DSVR is a quotient of two velocities.

We excluded several factors influencing DSVR measurement such as left ventricular hypertrophy, systemic hypertension, and myocardial infarction in this study. Other potential determinants of DSVR that were not measured and were not excluded in

this study may affect the physiologic estimates of the severity of LAD stenosis by our technique. Moreover, stenotic lesions other than the proximal LAD possibly affected our DSVR assessment. Further studies are needed that include patients with these variables.

Our method of physiologic assessment of coronary artery stenosis with TTDE is currently restricted to LAD for anatomic reasons. However, one randomized trial has shown that coronary artery bypass grafting improved survival of those with significant stenosis of the proximal portion of LAD in the 2- or 3-vessel coronary artery disease.[28] Accordingly, physiologic assessment of the severity of LAD stenosis can have a substantial clinical impact on the prognosis of patients with coronary artery disease.

Finally, we used exercise Tl-SPECT as a gold standard for assessing the physiologic severity of LAD stenosis. Indeed, there are not any reports that Tl-SPECT can reveal absolute physiologic severity of coronary stenosis. However, exercise TL-SPECT has been widely accepted as a method for physiologic estimates of the severity of coronary artery stenosis in routine clinical practice. Furthermore, many previous studies[10,23] have elucidated the usefulness of various parameters for the physiologic assessment of the severity of the coronary artery stenosis in comparison with exercise Tl-SPECT. Therefore, we believe that the use of exercise Tl-SPECT should be valid for our study design.

Clinical Implications

The fact that our procedure, compared with conventional methods, is totally noninvasive, inexpensive, and generally available, without any stress testing accompanied by the possibility of side effects, is considered an important advantage. It may provide additional information to physicians for making clinical decisions on the physiologic severity of coronary stenosis. It may also be useful for cases in which exercise stress testing cannot be performed.

Furthermore, stress echocardiography, including myocardial contrast echocardiography, for the diagnosis of coronary artery disease has recently gained increasing popularity. The assessment of DSVR during these stress echocardiograms is assumed to be available and must provide important diagnostic information for the physiologic estimate of the severity of LAD stenosis.

Conclusions

The measurement of DSVR by TTDE provides physiologic information concerning the severity of LAD stenosis without stress testing and the combination of contrast enhancement and high-frequency transducer allows high feasibility of this measurement with high success rate. This totally noninvasive method is free from the side effects of drugs and is useful for the clinical evaluation of myocardial ischemia.

REFERENCES

1. White CW, Wright CB, Doty DB, Hiratza LF, Eastham CL, Harrison DG, et al. Does visual interpretation of the coronary arteriogram predict the physiologic importance of a coronary stenosis? N Engl J Med 1984;310:819-24.
2. Marcus ML, Skorton DJ, Johnson MR, Collins SM, Harrison DG, Kerber RE. Visual estimates of percent diameter coronary stenosis: a battered gold standard. J Am Coll Cardiol 1988; 11:882-5.
3. Vogel RA. Assessing stenosis significance by coronary artriography: are the best variables good enough? J Am Coll Cardiol 1988;12:692-3.
4. Folts JD, Kahn DR, Bittar N, Rowe GG. Effects of partial obstruction on phasic flow in aortocoronary grafts. Circulation 1975;52(Suppl):I148-55.
5. Kajiya F, Tsujioka K, Ogasawara Y, Wada Y, Matsuoka S, Kanazawa S, et al. Analysis of flow characteristics in poststenotic regions of the human coronary artery during bypass graft surgery. Circulation 1987;76:1092-100.
6. Ofili EO, Kern MJ, Labovitz AJ, St Vrain JA, Segal J, Aguirre FV, et al. Analysis of coronary blood flow velocity dynamics in angiographically normal and stenosed arteries before and after endolumen enlargement by angioplasty. J Am Coll Cardiol 1993;21:308-16.
7. Ofili EO, Labovitz AJ, Kern MJ. Coronary flow velocity dymanics in normal and diseased arteries. Am J Cardiol 1993; 71:3-9D.
8. Segal J, Kern MJ, Scott NA, King SB III, Doucette JW, Heuser RR, et al. Alterations of phasic coronary artery flow velocity in humans during percutaneous coronary angioplasty. J Am Coll Cardiol 1992;20:276-86.
9. Segal J. Application of coronary flow velocity during angioplasty and other coronary interventional procedures. Am J Cardiol 1993;71:17-25D.
10. Deychak YA, Segal J, Reiner JS, Rohrbeck SC, Thompson MA, Lundergan CF, et al. Doppler guidewire flow-velocity indexes measured distal to coronary stenoses associated with reversible thallium perfusion defects. Am Heart J 1995;129: 219-27.
11. Donohue TJ, Kern MJ, Aguirre FV, Bach RG, Wolford T, Bell CA, et al. Assessing the hemodynamic significance of coronary artery stenoses: analysis of translesional pressure-flow velocity relations in patients. J Am Coll Cardiol 1993;22:449-58.
12. Piek JJ, Boersma E, di Mario C, Schroeder E, Vrints C, Probst P, et al, for the DEBATE study group. Angiographical and Doppler flow-derived parameters for assessment of coronary lesion severity and its relation to the result of the exercise electrocardiography. Eur Heart J 2000;21:466-74.
13. Crowley JJ, Shapiro LM. Analysis of phasic flow velocity dynamics in the left anterior descending coronary artery before and after angioplasty using transthoracic echocardiography in patients with stable angina pectoris. Am J Cardiol 1997;80:614-7.
14. Crowley JJ, Shapiro LM. Noninvasive analysis of coronary artery poststenotic flow characteristics by using transthoracic echocardiography. J Am Soc Echocardiogr 1998;11:1-9.
15. Higashiue S, Watanabe H, Yokoi Y, Takeuchi K, Yoshikawa J. Simple detection of severe coronary stenosis using transthoracic Doppler echocardiography at rest. Am J Cardiol 2001; 87:1064-8.

16. Caiati C, Montaldo C, Zedda N, Bina A, Iliceto S. New noninvasive method for coronary flow reserve assessment: contrast-enhanced transthoracic second harmonic echo Doppler. Circulation 1999;99:771-8.
17. Caiati C, Zedda N, Montaldo C, Montisci R, Iliceto S. Contrast-enhanced transthoracic second harmonic echo Doppler with adenosine: a noninvasive, rapid and effective method for coronary flow reserve assessment. J Am Coll Cardiol 1999;34: 122-30.
18. Hozumi T, Yoshida K, Ogata Y, Akasaka T, Asami Y, Takagi T, et al. Noninvasive assessment of significant left anterior descending coronary artery stenosis by coronary flow velocity reserve with transthoracic color Doppler echocardiography. Circulation 1998;97:1557-62.
19. Aragam JR, Main J, Guerrero JL, Vlahakes GJ, Southern JF, Adams MS, et al. Doppler color flow mapping of epicardial coronary arteries: initial observations. J Am Coll Cardiol 1993;21:478-87.
20. Gould KL, Lipscomb K. Effect of coronary stenoses on coronary flow reserve and resistance. Am J Cardiol 1974;34:48-55.
21. Rouleau J, Boerboom LE, Surjadhana A, Hoffman JI. The role of autoregulation and tissue diastolic pressure in the transmural distribution of left ventricular blood flow in anesthetized dog. Circ Res 1979;45:804-15.
22. Moses JW, Undermir C, Strain JE, Kreps EM, Higgins JE, Gleim GW, et al. Relation between single tomographic intravascular ultrasound image parameters and intracoronary Doppler flow velocity in patients with intermediately sever coronary stenoses. Am Heart J 1998;135:988-94.
23. Daimon M, Watanabe H, Yamagishi H, Muro T, Akioka K, Hirata K, et al. Physiologic assessment of coronary artery stenosis by coronary flow reserve measurements with transthoracic Doppler echocardiography: comparison with exercise thallium-201 single photon emission computed tomography. J Am Coll Cardiol 2001;37:1310-5.
24. Wilson RF, Wyche K, Christensen BV, Zimmer S, Laxson DD. Effects of adenosine on human coronary arterial circulation. Circulation 1990;82:1595-606.
25. Caiati C, Aragona P, Iliceto S, Rizzon P. Improved Doppler detection of proximal left anterior descending coronary artery stenosis after intravenous injection of a lung-crossing contrast agent: a transesophageal Doppler echocardiographic study. J Am Coll Cardiol 1996;27:1413-21.
26. Iliceto S, Caiati C, Aragona P, Verde R, Schlief R, Rizzon P. Improved Doppler signal intensity in coronary arteries after intravenous peripheral injection of a lung-crossing contrast agent (SHU 508A). J Am Coll Cardiol 1994;23:184-90.
27. Hozumi T, Yoshida K, Akasaka T, Asami Y, Ogata Y, Takagi T, et al. Noninvasive assessment of coronary flow velocity and coronary flow velocity reserve in the left anterior descending coronary artery by Doppler echocardiography: comparison with invasive technique. J Am Coll Cardiol 1998;32:1251-9.
28. European Coronary Surgery Study Group, Varnauskas E. Twelve-year follow-up of survival in the randomized European coronary surgery study. N Engl J Med 1988;319:332-7.

See related article, pages 663–673

Promotion of Cardiac Regeneration by Cardiac Stem Cells

Toshio Nagai, Ichiro Shiojima, Katsuhisa Matsuura, Issei Komuro

Research on myocardial regeneration is an exciting and promising area, which challenges the dogma that the heart is a nonregenerating organ. Recently, several methods of stem cell therapy have been developed. One method is to transplant cells into the infarcted area of the myocardium. Currently, clinical trials of autologous skeletal myoblast transplantation into the failed heart are underway and have been reported to improve the cardiac function.[1] However, the mechanism of its efficacy is unknown, and there are some questions about the safety because myoblasts do not transdifferentiate into cardiomyocytes and may induce lethal arrhythmia.[1] In this point, embryonic stem (ES) cells that can differentiate into cardiomyocytes are thought to be more promising.[2] For patients experiencing extensive myocardial infarction or dilated cardiomyopathy, however, the effectiveness of cell transplantation is questionable. Bone marrow–derived cells have been reported to transdifferentiate into various types of cells in situ. Indeed, bone marrow–derived stem cells were reported to prevent left ventricular remodeling after myocardial infarction and improve cardiac function by their differentiation into cardiomyocytes.[3] However, recent accumulating evidence has indicated that very few bone marrow cells, if any, transdifferentiate into cardiomyocytes.[4–6] Cytokine therapy using G-CSF strongly prevents ventricular remodeling after myocardial infarction by antiapoptotic and angiogenic effects, but not by recruitment of bone marrow cells.[7]

Over the past few years, adult hearts have been reported to contain the cardiac stem/progenitor cells such as c-kit+,[8] Sca-1+,[9,10] isl-1+,[11] and side population cells.[12] Because these cells have the ability to proliferate and differentiate into cardiomyocytes in vitro and in vivo, they might have the potential to regenerate the injured heart. However, there is almost no regeneration in the human heart after myocardial infarction, suggesting that cardiac regeneration accomplished by proliferation, migration, and differentiation of the cardiac stem/progenitor cells, is inhibited in vivo.

In this issue of *Circulation Research*, Urbanek et al address the possibility of cardiac regeneration by inducing migration and protection of cardiac stem cells and early committed cells (CSCs–ECCs) in a rodent myocardial infarction model.[13] CSCs are defined by the expression of the stem cell-related antigens, c-kit, Sca-1, or MDR1. A fraction of CSCs, which expressed MEF2C (cardiac transcription factor), GATA6 (smooth muscle cell transcription factor), or Ets-1 (endothelial cell transcription factor) was named ECCs. Immunohistochemical analysis revealed that CSCs–ECCs express HGF receptor c-Met and IGF-1 receptor (IGF-R) and, under the treatment with their ligands, cultured CSCs–ECCs secreted HGF/IGF-1. When myocardial infarction was produced and human HGF/IGF-1 was locally injected, expression levels of murine mRNA and proteins for HGF/IGF-1 in infarcted tissue were increased. Activation of these growth factor signals was confirmed by phosphorylation of c-Met, IGF-R, and their downstream targets. Migration studies demonstrated that HGF promoted motogenic and invasive activity of CSCs–ECCs, whereas IGF-1 had little effect. Conversely, IGF-1 showed more antiapoptotic and proliferative effects on CSCs–ECCs compared with HGF.

Based on these in vitro findings, Urbanek et al examined whether HGF/IGF-1 stimulate migration, proliferation, and differentiation of CSCs–ECCs in the infarcted heart. They used highly sophisticated techniques to evaluate the migration of CSCs–ECCs. They found that cycling CSCs–ECCs exist in the atrioventricular groove so that retrovirus expressing enhanced green fluorescent protein (EGFP) was injected in this region. After EGFP was integrated into the CSCs–ECCs, myocardial infarction was made and subsequently HGF/IGF-1 were injected into the predicted pathway of migrating cells with gradient of their concentration. They examined ex vivo heart preparation by 2 photon microscopy and demonstrated migration of EGFP-positive cells toward the infarcted area through the interstitium of the heart. Furthermore immunohistochemical analysis showed that the locomotive EGFP-positive cells possess the characteristics of CSCs–ECCs. Consistent with their in vitro data, HGF but not IGF-1 had locomotive effects on CSCs–ECCs. Regenerated myocardium after the HGF/IGF-1 combined treatment was identified as BrdU positive cardiomyocytes and vessels. HGF/IGF-1 treatment increased the number of newly-formed cells, resulting in an increased volume of myocardium, improvement of cardiac function, and better survival. The BrdU-positive new myocytes isolated from regenerated myocardium are smaller than old cells, and these small cells exhibit better contractile function than cardiomyocytes isolated from spared myocardium.

The same group has reported that self-renewing, clonogenic, and multipotent cardiac stem cells exist in the various species, including human[8,14,15]. However, in vivo kinetics of cardiac stem cells had been unknown because of the difficulty

From the Department of Cardiovascular Science and Medicine (T.N., I.S., K.M., I.K.), Chiba University Graduate School of Medicine, Chiba; and the Department of Cardiology (K.M.), Tokyo Women's Medical University, Tokyo, Japan.

Correspondence to Issei Komuro, MD, PhD, Department of Cardiovascular Science and Medicine, Chiba University Graduate School of Medicine, 1-8-1 Inohana, Chuo-ku, Chiba 260-8670, Japan. E-mail komuro-tky@umin.ac.jp

(*Circ Res.* **2005;97:615-617.**)

Circulation Research **is available at http://circres.ahajournals.org**
DOI: 10.1161/01.RES.0000186191.28820.34

of labeling and tracking of the cardiac stem cells in vivo. Urbanek et al overcame the difficulty by their extensive and skillful analyses and showed that exogenously-applied HGF induced migration of distant cardiac stem cells toward the infarcted area through the pathway defined by fibronectin. Despite the fact that many types of cytokines and growth factors, including HGF/IGF-1, were released in the ischemic myocardium, the resident stem cells cannot survive in infarcted myocardium, and the stem cells in the distant area do not take a part in regenerating heart tissue. The findings of this study suggest that the amount of the intrinsic factors are far less than the amount necessary to break the silence of the resident stem cells or protect them from apoptosis.

Although the study by Urbanek et al sheds light on intrinsic stem cell therapy by local administration of growth factors, it also raises several important questions that should be addressed by future studies. First, what determines the CSCs–ECCs quiescence in "cardiac niche"? In bone marrow niche, angiopoietin-1/Tie-2 signaling is critical for the maintenance of hematopoietic stem cell quiescence.[16] Although it is not clear whether the similar mechanism is present in the heart, it is possible that signals to maintain CSCs–ECCs quiescence are antagonized by HGF/IGF-1 signaling. CSCs–ECCs coexpress HGF/IGF-1 and c-Met/IGF-R, and there is a positive feedback loop of HGF/IGF-1 signaling in CSCs–ECCs. Therefore, CSCs–ECCs may exit from the quiescence when challenged by higher doses of HGF/IGF-1, and the activated state of CSCs–ECCs may be maintained by the positive feedback loop of HGF/IGF-1 signaling. Identification of the mechanism that maintains CSCs–ECCs quiescence will be of particular importance, because inhibition of CSCs–ECCs quiescence can be a novel strategy to promote myocardial regeneration by enhancing CSCs–ECCs proliferation. Second, how does HGF induce migration of CSCs–ECCs to the infarct area? Among several signaling molecules activated by HGF, PI3-kinase (PI3K) seems to be critical for HGF-mediated cell migration, because PI3K is required for HGF-induced lamellipodia formation and subsequent migration in MDCK and C2C12 cells.[17–19] Whether PI3K is also critical in CSCs–ECCs migration should be determined. In addition, it is possible that some negative regulators of CSCs–ECCs migration are expressed in the infarct area. Inhibition of such factors can be another strategy to promote myocardial regeneration. Third, what induces apoptosis of CSCs–ECCs in the infarct area? Small numbers of CSCs–ECCs migrate into infarct area without growth factor treatment. Understanding of the mechanism of the apoptosis would lead to more specific treatment by protecting stem cells. Finally, it is interesting to examine the effect of HGF/IGF-1 treatment in chronic heart failure models. In the study by Urbanek et al, animals were treated with growth factors 5 hours after coronary ligation. Whether administration of HGF/IGF-1 is also effective in the chronic stage after myocardial infarction, when ventricular remodeling is already established, should be investigated. Likewise, to determine whether growth factor treatment is also effective in dilated cardiomyopathy or other models of chronic heart failure with diffuse contractile dysfunction will be of great importance.

In summary, the study by Urbanek et al clearly demonstrates the therapeutic potential of CSCs–ECCs for myocardial regeneration. To address the questions raised by Urbanek et al would further advance our understanding of the stem cell system in the heart and provide important clues to the development of novel therapeutic strategies for heart diseases.

References

1. Menasche P, Hagege AA, Vilquin JT, Desnos M, Abergel E, Pouzet B, Bel A, Sarateanu S, Scorsin M, Schwartz K, Bruneval P, Benbunan M, Marolleau JP, Duboc D. Autologous skeletal myoblast transplantation for severe postinfarction left ventricular dysfunction. *J Am Coll Cardiol.* 2003;41:1078–1083.
2. Kofidis T, de Bruin JL, Yamane T, Tanaka M, Lebl DR, Swijnenburg RJ, Weissman IL, Robbins RC. Stimulation of paracrine pathways with growth factors enhances embryonic stem cell engraftment and host-specific differentiation in the heart after ischemic myocardial injury. *Circulation.* 2005;111:2486–2493.
3. Orlic D, Kajstura J, Chimenti S, Jakoniuk I, Anderson SM, Li B, Pickel J, McKay R, Nadal-Ginard B, Bodine DM, Leri A, Anversa P. Bone marrow cells regenerate infracted myocardium. *Nature.* 2001;410:701–705.
4. Balsam LB, Wagers AJ, Christensen JL, Kofidis T, Weissman IL, Robbins RC. Haematopoietic stem cells adopt mature haematopoietic fates in ischaemic myocardium. *Nature.* 2004;428:668–673.
5. Murry CE, Soonpaa MH, Reinecke H, Nakajima H, Nakajima HO, Rubart M, Pasumarthi KB, Virag JI, Bartelmez SH, Poppa V, Bradford G, Dowell JD, Williams DA, Field LJ. Haematopoietic stem cells do not transdifferentiate into cardiac myocytes in myocardial infarcts. *Nature.* 2004;428:664–668.
6. Nygren JM, Jovinge S, Breitbach M, Säwén P, Röll W, Hescheler J, Taneera J, Fleischmann BK, Jacobsen SEW. Bone marrow–derived hematopoietic cells generate cardiomyocytes at a low frequency through cell fusion, but not transdifferentiation. *Nat Med.* 2004;10:494–501.
7. Harada M, Qin Y, Takano H, Minamino T, Zou Y, Toko H, Ohtsuka M, Matsuura K, Sano M, Nishi J, Iwanaga K, Akazawa H, Kunieda T, Zhu W, Hasegawa H, Kunisada K, Nagai T, Nakaya H, Yamauchi-Takihara K, Komuro I. G-CSF prevents cardiac remodeling after myocardial infarction by activating the Jak-Stat pathway in cardiomyocytes. *Nat Med.* 2005;11:305–311.
8. Beltrami AP, Barlucchi L, Torella D, Baker M, Limana F, Chimenti S, Kasahara H, Rota M, Musso E, Urbanek K, Leri A, Kajstura J, Nadal-Ginard B, Anversa P. Adult cardiac stem cells are multipotent and support myocardial regeneration. *Cell.* 2003;114:763–776.
9. Oh H, Bradfute SB, Gallardo TD, Nakamura T, Gaussin V, Mishina Y, Pocius J, Michael LH, Behringer RR, Garry DJ, Entman ML, Schneider MD. Cardiac progenitor cells from adult myocardium: homing, differentiation, and fusion after infarction. *Proc Natl Acad Sci U S A.* 2003;100:12313–12318.
10. Matsuura K, Nagai T, Nishigaki N, Oyama T, Nishi J, Wada H, Sano M, Toko H, Akazawa H, Sato T, Nakaya H, Kasanuki H, Komuro I. Adult cardiac Sca-1-positive cells differentiate into beating cardiomyocytes. *J Biol Chem.* 2004;279:11384–11391.
11. Laugwitz KL, Moretti A, Lam J, Gruber P, Chen Y, Woodard S, Lin LZ, Cai CL, Lu MM, Reth M, Platoshyn O, Yuan JX, Evans S, Chien KR. Postnatal isl1+ cardioblasts enter fully differentiated cardiomyocyte lineages. *Nature.* 2005;433:647–653.
12. Martin CM, Meeson AP, Robertson SM, Hawke TJ, Richardson JA, Bates S, Goetsch SC, Gallardo TD, Garry DJ. Persistent expression of the ATP-binding cassette transporter, Abcg2, identifies cardiac SP cells in the developing and adult heart. *Dev Biol.* 2004;265:262–275.
13. Urbanek K, Rota M, Cascapera S, Bearzi C, Nascimbene A, Angelis AD, Hosoda T, Chimenti S, Baker M, Limana F, Nurzynska D, Torella D, Rotatori F, Rastaldo F, Musso E, Quaini F, Leri A, Hintze TH, Kajstura J, Anversa P. Cardiac stem cell possesses the growth factor-receptor system that following activation the regenerative the infarcted myocardium improving ventricular function and long term survival. *Circ Res.* 2005;97:663–673.

14. Chimenti C, Kajstura J, Torella D, Urbanek K, Heleniak H, Colussi C, Di Meglio F, Nadal-Ginard B, Frustaci A, Leri A, Maseri A, Anversa P. Senescence and death of primitive cells and myocytes lead to premature cardiac aging and heart failure. *Circ Res.* 2003;93:604–613.
15. Messina E, Angelis LD, Frati G, Morrone S, Chimenti S, Fiordaliso F, Salio M, Battaglia M, Latronico MVG, Coletta M, Vivarelli E, Frati L, Cossu G, Giacomello A. Isolation and expansion of adult cardiac stem cells from human and murine heart. *Circ Res.* 2004;95:911–921.
16. Arai F, Hirao A, Ohmura M, Sato H, Matsuoka S, Takubo K, Ito K, Koh GY, Suda T. Tie2/angiopoietin-1 signaling regulates hematopoietic stem cell quiescence in the bone marrow niche. *Cell.* 2004;118:149–161.
17. Khwaja A, Lehmann K, Marte BM, Downward J. Phosphoinositide 3-kinase induces scattering and tubulogenesis in epithelial cells through a novel pathway. *J Biol Chem.* 1998;273:18793–18801.
18. Royal I, Lamarche-Vane N, Lamorte L, Kaibuchi K, Park M. Activation of cdc42, rac, PAK, and rho-kinase in response to hepatocyte growth factor differentially regulates epithelial cell colony spreading and dissociation. *Mol Biol Cell.* 2000;11:1709–1725.
19. Kawamura K, Takano K, Suetsugu S, Kurisu S, Yamazaki D, Miki H, Takenawa T, Endo T. N-WASP and WAVE2 acting downstream of phosphatidylinositol 3-kinase are required for myogenic cell migration induced by hepatocyte growth factor. *J Biol Chem.* 2004;279:54862–54871.

KEY WORDS: cardiac stem cell ■ cardiomyocytes ■ regeneration ■ growth factor ■ myocardial infarction

Pulmonary Vein Morphology Before and After Segmental Isolation in Patients with Atrial Fibrillation

MAREHIKO UEDA,* HIROSHI TADA,† KENJI KUROSAKI,† KAZUHIRO ITOI,‡ KEIKO KOYAMA,‡ SHIGETO NAITO, † SACHIKO ITO, † ISSEI KOMURO,* SHIGERU OSHIMA,† and KOICHI TANIGUCHI†

From the *Department of Cardiovascular Science and Medicine, Chiba University Graduate School of Medicine, Chiba, Japan, and †Divisions of Cardiology and ‡Radiology, Gunma Prefectural Cardiovascular Center, Maebashi, Gunma, Japan

UEDA, M., ET AL.: Pulmonary Vein Morphology Before and After Segmental Isolation in Patients with Atrial Fibrillation. ***Background:*** *The morphology of the pulmonary veins (PVs) before and after segmental isolation of the PVs has not been sufficiently characterized.*

Methods and Results: *Multi-slice computed tomography was performed before and 3 ± 1 months after ablation in 30 patients with atrial fibrillation who underwent PV isolation. Before ablation, PV narrowing (≥25% luminal reduction) was found in nine (8%) PVs. After ablation, de novo PV narrowing was found in 24 PVs (26%) and was detected only in the supero-inferior direction in 14 PVs (58%). The diameter reduction inside the PVs after ablation was greater in the supero-inferior direction (14 ± 12%) than in the antero-posterior direction (9 ± 13%; P < 0.0001). In the ablated PVs, the PV trunk was shorter than before ablation (P < 0.0001). The reduction in the diameters of both the PV ostium and the ablation site in the ablated PVs, as well as the diameter of the PV ostium in the nonablated PVs, correlated with the decrease in the left atrial diameter. Shortening of the PV trunk correlated with the severity of PV narrowing, but it was not related to the percent diameter reduction of the left atrium. PV narrowing before or after ablation did not result in any clinical consequences.*

Conclusions: *PV narrowing is present in about 10% of PVs before ablation. Asymmetric luminal reduction and longitudinal shrinkage of the PV trunk occur after ablation. Reverse remodeling of the PV and contraction of the PV wall may contribute to the reduction in the PV diameter. PV morphology should be assessed with multi-directional views to avoid missing heterogeneous legions. (PACE 2005; 28:944–953)*

atrial fibrillation, catheter ablation, radiology

Introduction

Segmental ostial ablation to isolate the pulmonary veins (PV isolation) has been demonstrated to be effective in curing atrial fibrillation (AF).[1,2] However, radiofrequency (RF) energy delivery in the PVs is associated with the development of PV stenosis.[3–6] The morphology of the PVs and anatomical alternation after RF ablation have been investigated using magnetic resonance imaging and computed tomography (CT).[4–7] However, a detailed and quantitative analysis of the PV morphology after ablation using multi-directional views has not been performed. Furthermore, the presence and incidence of PV narrowing before ablation or longitudinal PV shrinkage after ablation has not yet been examined. It is well known that AF can induce structural remodeling of the atria and cause atrial enlargement, which may be reversible if AF is converted and sinus rhythm maintained (reverse remodeling).[4,5] However, reverse remodeling of the PVs after ablation has not been sufficiently demonstated. The purpose of this study was to clarify those points.

Methods

Study Patients

This study included 30 patients with drug-resistant, paroxysmal AF (24 men, 6 women; mean age, 59 ± 8 years). The mean AF duration was 7 ± 7 years, and the mean number of symptomatic AF episodes per month was 20 ± 22. Echocardiography demonstrated a mean left ventricular ejection fraction of 0.63 ± 0.09. Two patients had coronary artery disease and the remaining 28 had no structural heart disease. In 10 patients (33%), linear ablation of the cavo-tricuspid isthmus was also performed for typical atrial flutter at the time of PV isolation. Multi-slice CT was performed within 1 week before and 3 ± 1 months after the PV isolation. At the time of acquisition of the CT before and after the PV isolation, all patients were in normal

This work was supported by a Research Grant for Cardiovascular Diseases (14C-2) from the Ministry of Health, Labor, and Welfare, Japan.

Address for reprints: Hiroshi Tada, M.D., Division of Cardiology, Gunma Prefectural Cardiovascular Center, 3-12 Kameizumi, Maebashi, Gunma 371-0004, Japan. Fax: 81-027-269-1492; e-mail: tada.h@cvc.pref.gunma.jp

Received February 10, 2005; revised April 14, 2005; accepted June 1, 2005.

sinus rhythm. All patients gave informed consent for an electrophysiologic study, catheter ablation, and CT. As a control group, CT also was performed in 14 subjects with neither a history of AF nor structural heart disease (10 men, 4 women; mean age, 57 ± 16 years).

Electrophysiologic Study and Catheter Ablation

PV isolation was performed as previously described.[1,2,8] Electrograms were recorded near the PV ostia with a 7 Fr decapolar ring catheter (Lasso, Biosense Webster, Inc., Diamond Bar, CA, USA). RF energy was delivered with a 7 Fr quadripolar ablation catheter with a 4 mm distal electrode. PV isolation was performed by applying RF energy at the sites at which the earliest bipolar PV potentials and/or unipolar electrograms with the most rapid intrinsic deflection were recorded.[1,2,8] RF energy was delivered at a maximum power of 30 W and maximum temperature of 52°C–55°C for 60 seconds.[1,2,8] The endpoint for ablation was the elimination of the PV potentials at all Lasso catheter recording sites.

Multi-Slice CT

The images were acquired using a multi-slice CT scanner (GE Light Speed Ultra; GE Medical Image, Milwaukee, WI, USA) during intravenous injection of contrast dye (100 mL at 3 mL/s) in eight parallel slices (1.25 mm collimation). ECG gating was performed with a triggered delay set at 70% of the R-to-R interval to target the atrial end-diastolic phase. A processing workstation (Advanced Workstation 4.0; GE Medical Image) allowed for three-dimensional viewing of curved multi-planar reconstruction (MPR) images (Fig. 1A and B), virtual endoscopic images, reformatted cross-sectional images in discretionary directions (Fig. 1C), and volume rendering images (Figs. 2, upper panels, and 3). Curved MPR images were obtained using a cursor to trace a curved line along the center of the lumen of the PV manually on

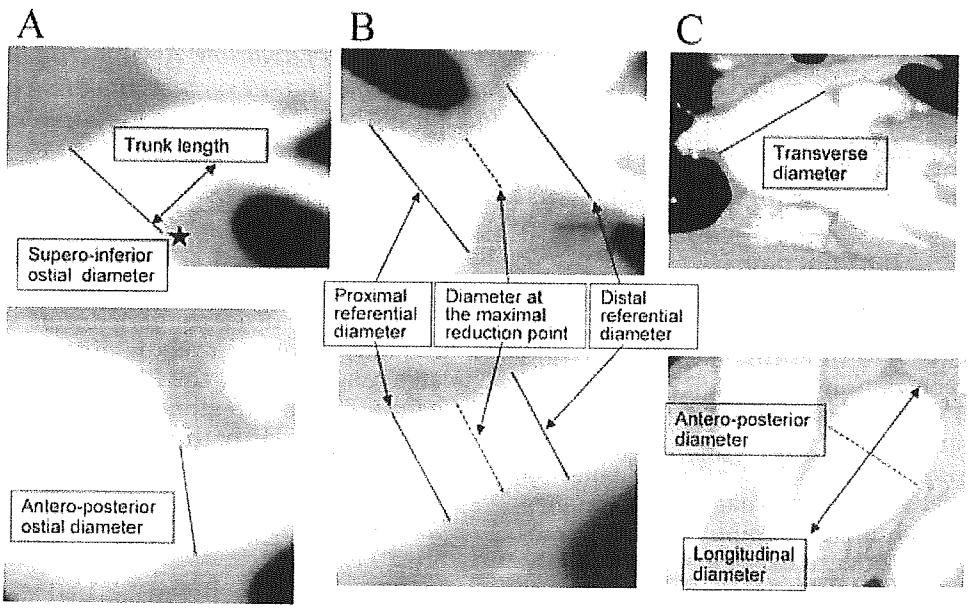

Figure 1. *(A) Measurement of the ostia of the pulmonary veins (PV) with curved MPR (upper panel: integrated coronal sectional view) and axial (lower panel: integrated axial sectional view) images of the left superior PVs. The black asterisk identifies the apex of the parabolic outline of the junction of the intervenal bridging wall. The trunk length of the PV was defined as the distance between the ostium and the onset of the first branch of the PV (arrow). The white asterisk identifies the apex of the parabolic outline of the junction to the left atrial appendage. (B) Coronal sectional (upper panel) and axial sectional (lower panel) images of the left superior PV demonstrating asymmetric stenosis after ablation. The full and dotted lines indicate the diameters of the peri-lesion references and the point of the maximal luminal reduction, respectively. This PV has a 48% luminal reduction in the supero-inferior direction (upper panel), but only a 14% luminal reduction in the antero-posterior direction (lower panel), indicating a heterogeneous pattern of stenosis in this vein. (C) Measurement of the left atrial diameters. The transverse (full line), antero-posterior (dotted line), and longitudinal diameters (arrow) were measured.*

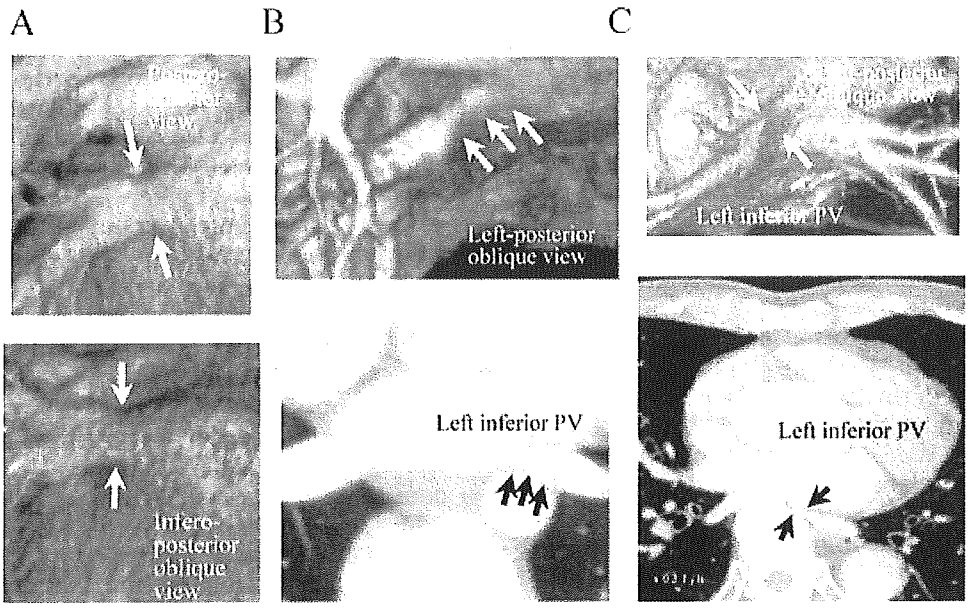

Figure 2. *(A) Volume rendering images of the left inferior pulmonary vein (PV) in a patient with atrial fibrillation before ablation. The arrows indicate a narrowing of the vein (27% luminal reduction). (B) A volume rendering image postprocessing cutting the descending aorta (upper panel) and curved MPR (lower panel) of the left inferior PV before ablation. Dominant luminal reduction on the posterior side is shown. (C) A volume rendering image of the left inferior PV postprocessing cutting the spine (upper panel) and axial cross-sectional CT image (lower panel) in a control patient. The arrows indicate the narrowest portion of the vein (66% luminal reduction). A narrowed and kinked left inferior PV, positioned between the left atrium and the spine, is shown (black arrows).*

carefully selected cross-sectional source images, and orthogonal to the source images.[9]

Measurements and Analysis

In 30 patients with AF, quantitative measurements of the PVs, using electronic three-dimensional digital calipers, were performed in the right superior (n = 30; RS), right inferior (n = 30; RI), left superior (n = 26; LS), and left inferior (n = 26; LI) PVs (Fig. 1). Four obvious left common PVs and three right middle PVs that were found were excluded from the analysis. The PV ostial diameter was measured in two orthogonal directions (antero-posterior and supero-inferior directions; Fig. 1A). One of the ends of the digital caliper was set at the geometric junction (i.e., inflection or apex of the parabolic outline) between the PV and the intervenal bridging wall for the supero-inferior measurement or anterior wall of the left atrium (LA) or LA appendage for the antero-posterior measurement (Fig. 1A). The intersection of the opposite wall with a line perpendicular to

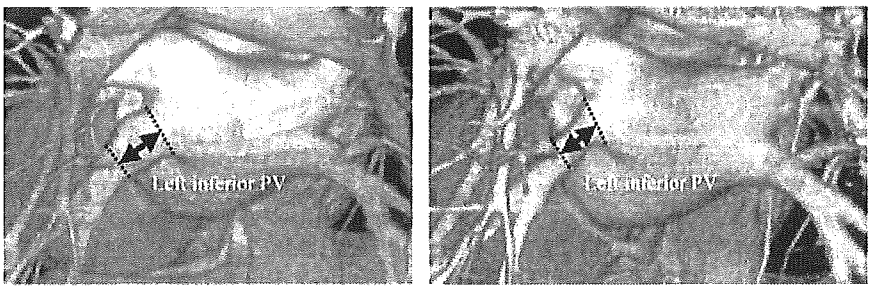

Figure 3. *Volume rendering images of the left inferior pulmonary vein (PV) before (left panel) and after ablation (right panel). The trunk length of the PV shortened after ablation (23% reduction compared with that before ablation).*

the trunk axis running from the aforementioned junction was used as the other end for the measurement (Fig. 1A).

When a luminal reduction inside the PV was visualized on the curved MPR image, the severity of the luminal reduction was assessed as the percent diameter reduction inside the PV with a referential diameter that was the average of the distal and proximal peri-lesion diameters (Fig. 1B). After measuring the luminal reduction in two orthogonal directions, the larger of the percent diameter reduction values was used as the severity of the luminal reduction.We set 0% for the percent diameter reduction of the PVs without a luminal reduction. A luminal reduction $\geq$25% was defined as PV narrowing. We distinguished a *de novo* luminal reduction in the ablated PV from the pre-existent luminal reduction that was visualized both before and after ablation using the bidirectional curved MPR. In the PV without a pre-existent luminal reduction, we determined the luminal reduction that could be visualized after ablation to be a *de novo* luminal reduction. In the PVs with a pre-existent luminal reduction, an alteration $\geq$2 mm in the distance from the PV ostium to the narrowest point, conversion to tandem lesions from a single lesion, conversion to a bidirectional lesion from a unidirectional lesion, or increase $\geq$15% in the luminal reduction was defined as emergence of a *de novo* luminal reduction. The narrowest portion of the *de novo* luminal reduction was defined as the ablation site. The distance between the estimated ablation site and the PV ostium before ablation was calculated as (distance between the point of the maximal diameter reduction and the PV ostium $\times$ length of the PV trunk before ablation/length of the PV trunk after ablation). The diameter of the estimated ablation site before ablation was measured on the first CT image. The percent change in the diameter of the ablation site also was calculated as (100 − 100 $\times$ diameter of the ablation site after ablation/diameter of the estimated ablation site before ablation).

The length of the PV trunk, which was defined as the distance from the ostium to the first branching point of the PV, was measured in the coronal sectional view (Fig. 1A). The antero-posterior, supero-inferior, and transverse diameters of the LA were also measured before and after ablation (Fig. 1C). The transverse diameter of the LA was measured between the ostia of the superior PVs on the oblique coronal section. The antero-posterior diameter was measured at the level of the sino-tubular junction on the oblique sagittal section. The longitudinal diameter was measured from the roof to the mitral annulus on the oblique sagittal section. The percent diameter reduction of the PV ostium and LA was calculated as (100 − 100 $\times$ diameter before ablation/diameter after ablation).

All ablation sites were verified using multiplane fluoroscopy, and each ablation site was assessed using the 12 divided segments of the PV wall (Fig. 4A), and the extent of the circumferential ablation area and number of RF energy deliveries in the four anatomic segments of the PV (superior, inferior, anterior, and posterior segments; Fig. 4B) were obtained.

Statistical Analysis

Continuous variables are expressed as mean $\pm$ SD. Continuous variables were compared with the *t*-test or one-way ANOVA coupled with Scheffe's test, as appropriate. Categorical variables were compared using the Fisher's exact test. Correlations between variables were assessed by Pearson's linear correlation and tested using Fisher's *z* transformation. All statistical analyses were carried out using the Stat-View statistical package, version 5.0 (Abacus Concept, Inc., Berkeley, CA, USA). A P value < 0.05 was considered statistically significant.

Results

PV and LA Characteristics in Patients with AF Before Ablation

The supero-inferior diameter of the PV ostium was greater than the antero-posterior ostial diameter in each of the PVs ($P < 0.0001$ for each; Table I). The supero-inferior ostial diameter did not differ among the four PVs, but the antero-posterior ostial diameter of the LIPV was smaller than the other three PVs ($P < 0.05$ for each). The supero-inferior and antero-posterior diameters of the ostium in the AF patients were greater than those in the control subjects (Table I). However, the trunk length of each PV in the AF patients (12.9 $\pm$ 7.6 mm) did not differ from the control subjects (11.9 $\pm$ 7.4 mm, $P = 0.4$). The transverse and antero-posterior LA diameters were greater in the AF patients than in the control subjects (Table I).

Luminal Reduction of the PVs Before Ablation

A luminal reduction in the PVs was observed in patients with AF before ablation as well as in the control subjects. In patients with AF, the average luminal reduction of all 112 PVs that were assessed was 6 $\pm$ 10% (range, 0–34), and the distance from the ostium to the narrowest point in the PV was 6.7 $\pm$ 3.9 mm in the supero-inferior direction and 7.1 $\pm$ 4.6 mm in the antero-posterior direction. A luminal reduction was frequently observed and its severity was the greatest in the LIPV among the four PVs (Table II). PV narrowing was found in nine (8%) PVs (eight LIPVs and one LSPV; Table II,

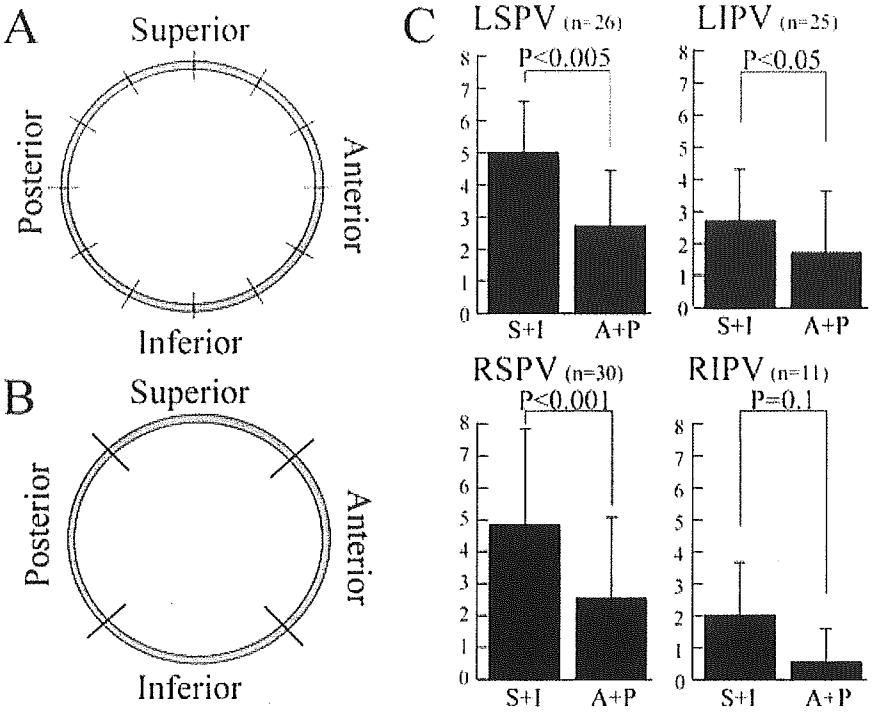

Figure 4. *(A) A representation of the pulmonary vein (PV) divided into 12 segments for calculating the circumferential ablation region. (B) A representation of the PV divided into four segments to assess the number of RF energy deliveries at the four anatomic segments of the PV. (C) Total number of RF energy applications at the superior and inferior segments (S + I) and at the anterior and posterior (A + P) segments within the PV. LI (S) = left inferior (superior); RI (S) = right inferior (superior).*

Fig. 2A and B). Four of the PV narrowings (44%) were found only in the antero-posterior direction, but no PV narrowings were found only in the supero-inferior direction.

In the control subjects, the average luminal reduction was 5.8 ± 13% (range, 0–66%), and PV narrowing was found in six LIPVs (10%). A control subject with mild pectus excavatum had a 66% luminal reduction (Fig. 2C). There were no differences in the incidence or severity of segmental PV narrowing between the AF patients and the control subjects. Inside the LIPVs, six of the eight narrowings (75%) in the AF patients and four of the six narrowings (67%) in the control subjects were dominant on the posterior side adjacent to the descending aorta (Fig. 2B).

Ablation Procedure

RF energy was delivered at the 92 PVs (30 RSPVs, 11 RIPVs, 26 LSPVs, and 25 LIPVs) and complete electrical isolation was achieved in 88 (96%) PVs. In each of the PVs, RF energy was delivered more often at the superior and inferior segments than at the anterior and posterior segments (Table III, Fig. 4C). No complications occurred during the ablation procedures.

Status of the Patients up to the Time of the Second CT

After ablation, 18 patients (60%) had no AF recurrence without the use of antiarrhythmic drugs. In the remaining 12 patients (40%), AF recurred within 1 week after ablation, and they were treated with class I or class III antiarrhythmic drugs that had been ineffective before ablation and they subsequently had no symptomatic AF episodes. No patients had any symptoms from the PV narrowing. At the second CT scanning, no patients had varied ≥5% in the ratio of the "R-to-P interval" to the "R-to-R interval" compared to the first scanning.

Luminal Reduction Inside the PV After Catheter Ablation

After PV isolation, a *de novo* luminal reduction was present in 53 ablated PVs (58%; range, 5–46%), and the average severity of the *de novo* luminal reduction in all 92 ablated PVs, including 39 PVs with no *de novo* luminal reduction (severity = 0%), was 16 ± 14%. The percent diameter reduction of the *de novo* luminal reduction was greater in the supero-inferior direction (14 ±

Table I.

Measured Diameters of the Pulmonary Vein Ostia and Left Atrium in Patients with Atrial Fibrillation and Control Subjects

A. Pulmonary Vein	AF Patients Before Ablation	Ablated PVs of the AF patients		Control Subjects	P Value 1	P Value 2
		Before	After			
LSPV Number	26		26	15		
Supero-inferior diameter (mm)	21.1 ± 3.0	21.1 ± 3.0	18.7 ± 2.9	20.1 ± 3.1	<0.0001	0.3
Antero-posterior diameter (mm)	17.2 ± 2.9	17.2 ± 2.9	15.3 ± 2.6	15.1 ± 2.8	<0.0001	<0.05
SI/AP	1.24 ± 0.17	1.24 ± 0.17	1.24 ± 0.16	1.35 ± 0.17	0.8	0.07
RSPV Number	30		30	15		
Supero-inferior diameter (mm)	21.6 ± 2.7	21.6 ± 2.7	17.6 ± 2.8	19.7 ± 2.9	<0.0001	<0.05
Antero-posterior diameter (mm)	17.7 ± 2.8	17.7 ± 2.8	16.3 ± 2.6	15.5 ± 2.6	<0.001	<0.05
SI/AP	1.24 ± 0.33	1.24 ± 0.33	1.22 ± 0.20	1.28 ± 0.19	0.4	0.5
LIPV Number	26		25	15		
Supero-inferior diameter (mm)	20.6 ± 3.1	20.5 ± 3.1	18.9 ± 3.0	18.2 ± 2.9	<0.0005	<0.05
Antero-posterior diameter (mm)	14.9 ± 2.8	14.9 ± 2.8	13.9 ± 2.5	12.8 ± 3.0	<0.0005	<0.05
SI/AP	1.37 ± 0.18	1.37 ± 0.18	1.39 ± 0.20	1.50 ± 0.29	0.8	0.3
RIPV Number	30		11	15		
Supero-inferior diameter (mm)	20.4 ± 2.8	19.8 ± 2.2	19.3 ± 1.8	19.1 ± 2.5	0.2	0.1
Antero-posterior diameter (mm)	16.4 ± 2.3	17.0 ± 1.5	16.4 ± 1.6	14.3 ± 2.6	0.06	<0.01
SI/AP	1.26 ± 0.18	1.17 ± 0.16	1.18 ± 0.16	1.39 ± 0.37	0.6	0.09

B. Left Atrium	Control Subjects	AF Patients		P Value 1	P Value 2
		Before	After		
Number	15		30		
Traverse diameter (mm)	48.0 ± 5.0	55.6 ± 6.8	53.2 ± 6.2	<0.0005	<0.001
Longitudinal diameter (mm)	64.0 ± 7.5	66.1 ± 7.9	63.9 ± 8.6	<0.005	0.4
Antero-posterior diameter (mm)	31.7 ± 6.2	37.7 ± 7.7	35.6 ± 7.6	<0.0001	<0.05

Values are mean ± standard deviation. AF = atrial fibrillation; LI (S) = left inferior (superior); PV = pulmonary vein; RI(S) = right inferior (superior); SI/AP = ratio of supero-inferior diameter to antero-posterior diameter. p value 1: before ablation vs. after ablation (paired t test), p value 2: the AF patients before PV isolation vs. the control subjects (non-paired t test).

12%) than in the antero-posterior direction (9 ± 13%, P < 0.0001; Table II and Figs. 1B and 5), but the severity of the PV stenosis in the antero-posterior direction was greater than in the supero-inferior direction in 14% of ablated PVs. *De novo* PV narrowing after ablation was found in 24 PVs (26%; Table II). It could be detected in both directions in 10 PVs (42%), but was detected only in the supero-inferior direction in the remaining 14 PVs (58%; Fig. 1B). No *de novo* PV narrowing was found only in the antero-posterior direction. Four PVs which had PV narrowing before ablation demonstrated *de novo* PV narrowing after ablation. These were all LIPVs, and it occurred at a proximal site to the site with pre-existent PV narrowing in three LIPVs and at the site with pre-existent PV narrowing in the remaining one LIPV.

The severity of the *de novo* luminal reduction was greater and the incidence of the *de novo* narrowing was higher in the left PVs than the right PVs, and the LIPV had the greatest severity of luminal reduction and the highest incidence of *de novo* narrowing among the four PVs (Table II). The distance between the PV ostium and the site showing the maximal diameter reduction of the *de novo* luminal reduction was 6.0 ± 3.3 and 5.6 ± 3.2 mm in the coronal and axial sectional views, respectively. The distance between the distal and proximal referential points (length of the luminal reduction) was 9.7 ± 2.2 mm in the supero-inferior direction and 9.8 ± 2.1 mm in the antero-posterior direction.

Diameter Reduction at the Ostium of the PV After Catheter Ablation

In the LSPV, RSPV, and LIPV, the supero-inferior and antero-posterior diameters of the PV ostium after ablation were smaller than those

Table II.

Percent Diameter Reduction and Its Severity for the Pulmonary Veins and the Incidence of the Narrowing of the Pulmonary Vein Before and After Ablation

	%Diameter Reduction			
	Supero-Inferior	Antero-Posterior	Severity (%)	Incidence of PV Narrowing (%)
Preexistent luminal reduction before ablation				
LSPV	3.7 ± 7.4	2.0 ± 6.0	4.4 ± 7.9	1/26 (4%)
RSPV	2.1 ± 5.4	0 ± 0	2.1 ± 5.4	0/30 (0%)
LIPV	8.0 ± 11.0	11.7 ± 13.6	16.0 ± 12.3†	8/26 (31%)*
RIPV	0.7 ± 4.0	0.9 ± 5.2	1.7 ± 6.4	0/30 (0%)
De novo luminal reduction after ablation				
LSPV	18.5 ± 10.0	10.8 ± 11.5	19.6 ± 10.5	9/26 (35%)
RSPV	10.1 ± 11.1	3.0 ± 6.6	10.3 ± 11.0	3/30 (10%)
LIPV	20.4 ± 12.9	18.4 ± 15.3	24.5 ± 14.0	12/25 (48%)
RIPV	1.1 ± 3.8	0 ± 0	1.1 ± 3.8	0/11 (0%)

Values are mean ± standard deviation. After measurement of the %diameter reduction in two orthogonal directions (supero-inferior and antero-posterior directions), the greater value for the %diameter reduction was chosen for a severity of luminal reduction. LI (S) = left inferior (superior); PV = pulmonary vein; RI (S) = right inferior (superior). *P < 0.05, †P < 0.005, ‡P < 0.0005.

before ablation (P < 0.001 for all; Table I). Both the supero-inferior and antero-posterior percent diameter reductions in the PV ostium correlated with the severity of the *de novo* luminal reduction (r = 0.31, P < 0.01 and r = 0.30, P < 0.01, respectively). In the 20 non-ablated PVs (19 RIPVs and 1 LIPV), both diameters of the PV ostium after ablation were also smaller than those before ablation (Fig. 6A).

Longitudinal Shrinkage of the Ablated PVs

In the ablated PVs, the PV trunk after ablation (12.2 ± 7.6 mm) was shorter than before ablation (13.4 ± 8.1 mm, P < 0.0001; Figs. 3 and 6B). The average percent shortening of the PV trunk was 8.4 ± 10.2% (range, −5% to 34%). Shortening of the PV trunk correlated with the severity of the *de novo* luminal reduction inside the PV (r = 0.40, P < 0.0005), but it was not related to the percent diameter reduction of the LA (r = 0.15, P = 0.14 for transverse; r = 0.21, P = 0.056 for longitudinal; and r = −0.14, P = 0.22 for antero-posterior percent diameter reduction of the LA). In the non-ablated PVs, the trunk length did not change after ablation (P = 0.07; Fig. 6B).

Table III.

Distribution of the Ablated Area Where RF Energy Was Delivered in the Pulmonary Vein

	Number of RF Energy Application					Ablated Area in the PV	Total Amounts of RF Energy (J)
	Superior	Inferior	Anterior	Posterior	Total		
LSPV	1.9 ± 1.3	3.1 ± 2.0	1.5 ± 1.3	1.2 ± 1.2	7.7 ± 3.3	0.49 ± 0.16	13,617 ± 7,996
RSPV	2.6 ± 1.5	2.3 ± 2.1	1.2 ± 1.5	1.3 ± 1.3	7.3 ± 4.6	0.50 ± 0.15	13,301 ± 6,552
LIPV	1.7 ± 1.2	1.1 ± 1.2	0.8 ± 1.1	0.8 ± 1.3	4.4 ± 2.9	0.39 ± 0.22	6,246 ± 4,285
RIPV	1.3 ± 1.4	0.8 ± 1.0	0.1 ± 0.4	0.4 ± 0.7	2.5 ± 1.3	0.26 ± 0.21	3,099 ± 2,510
Total	2.0 ± 1.4	2.1 ± 2.0	4.1 ± 2.7	1.0 ± 1.2	6.2 ± 4.0	0.48 ± 0.50	10,680 ± 7,887

Values are mean ± standard deviation. LI (S) = left inferior (superior); n = number; PV = pulmonary vein; RI(S) = right inferior (superior). *P < 0.05, †P < 0.005, ‡P < 0.0005.